Sensitivity enhancement of a high-resolution negative-tone nonchemically amplified metal organic photoresist for extreme ultraviolet lithography

Scott M. Lewis,[a,b,c,*] **Hayden R. Alty**,[a] **Michaela Vockenhuber**,[d] **Guy A. DeRose**,[b] **Antonio Fernandez-Mato**,[a] **Dimitrios Kazazis**,[d] **Paul L. Winpenny**,[c] **Richard Grindell**,[c] **Grigore A. Timco**,[a] **Axel Scherer**,[b] **Yasin Ekinci**,[d] **and Richard E. P. Winpenny**[a,c]

[a]University of Manchester, School of Chemistry and Photon Science Institute, Manchester, United Kingdom

[b]Kavli Nanoscience Institute, California Institute of Technology, Pasadena, California, United States

[c]Sci-Tron Ltd., Walsall, United Kingdom

[d]Paul Scherrer Institute, Advanced Lithography and Metrology Group, Villigen, Switzerland

Abstract. A new class of negative-tone resist materials has been developed for electron beam and extreme ultraviolet lithography. The resist is based on heterometallic rings. From initial electron beam lithography studies, the resist performance demonstrated a resolution of 40-nm pitch but at the expense of a low sensitivity. To improve the sensitivity, we incorporated $HgCl_2$ and HgI_2 into the resist molecular design. This dramatically improved the resist sensitivity while maintaining high resolution. This improvement was demonstrated using electron beam and extreme ultraviolet lithography. © *2022 Society of Photo-Optical Instrumentation Engineers (SPIE)* [DOI: 10.1117/1.JMM.21.4.041404]

Keywords: metal organic EUV photoresist; metal organic electron beam resist; extreme ultraviolet lithography; electron beam lithography.

Paper 22007SS received Feb. 9, 2022; accepted for publication May 4, 2022; published online Jun. 2, 2022.

1 Introduction

The ability to produce patterns at the nanoscale using lithography underpins modern society. The electronic devices we take for granted contain integrated circuits (IC) and the key component of those ICs are field-effect transistors (FETs). They have reduced in size by a factor of two every 2 years for over 50 years, following Moore's law. The roadmap for the electronics industry now assumes that this constant reduction of size will continue—at least until the mid-2020s.[1] However, there is a significant challenge now as the feature size drops to 20 nm and below. At the end of 2019, extreme ultraviolet lithography (EUVL) was adopted to manufacture FinFETs (i.e., multigate FETs where the gates wrap around fin-like channels) that are an integral part of today's ICs at the 7-nm node and beyond. As future technology nodes will take full advantage of the EUVL technique, it will become increasingly challenging to transfer the patterns into the silicon with existing organic resist materials. This is because as the resolution of the pattern increases, the aggressive conditions of the etch plasma will need to be increased substantially, leading to a decrease in etch efficiency.[2,3] Therefore, inorganic resist materials, which provide superior etch selectivity, must be explored.

In a previous study, we reported a negative-tone resist that is based on a metal–organic compound.[2] This resist produced line and space patterns of 20-nm half-pitch (HP) resolution, while demonstrating extraordinary silicon dry etch performance of $>100:1$ selectivity.

*Address all correspondence to Scott M. Lewis, scott.lewis@manchester.ac.uk; slewis2@caltech.edu

1932-5150/2022/$28.00 © 2022 SPIE

Downloaded From: https://www.spiedigitallibrary.org/journals/Journal-of-Micro/Nanopatterning,-Materials,-and-Metrology on 07 Jun 2022
Terms of Use: https://www.spiedigitallibrary.org/terms-of-use

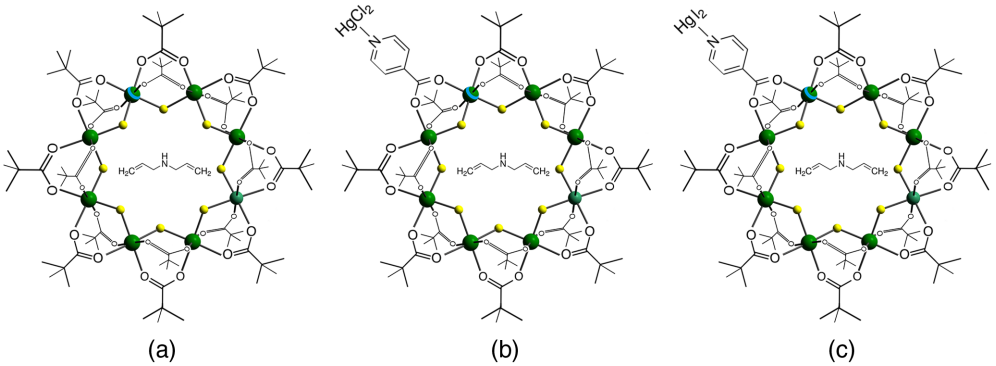

Fig. 1 The structures of compounds in the crystal: (a) resist **1**, (b) resist **2**, and (c) resist **3**. Cr green, Ni green with a blue band, F yellow, H atoms omitted for clarity.

Unfortunately, this was produced at the expense of resist sensitivity, where the exposure dose was 61,000 $\mu C/cm^2$ for electron beam lithography (EBL). Although the sensitivity is very low, it shows great promise from a pattern transfer point of view. Therefore, this resist could provide an excellent framework to easing the challenges of dry etching in future technology nodes.

From this, we have used our three-dimensional (3D) Monte Carlo simulator to improve the resist sensitivity without losing the pattern resolution. This gave a critical understanding of the exposure mechanism, which allowed the exposure efficiency of the resist to be increased.[4,5] This has led us to hypothesize that by incorporating both the diallylammonium at the center of the molecule [see Fig. 1(a)] and the addition of heavy metal salts on the outside of the molecule [see Figs. 1(b) and 1(c)] would lead to further gains in sensitivity. It is well known that secondary electrons (SEs) are essential to lowering the exposure dose for EBL as these electrons are responsible for exposing the resist.[6] The results from our model show that the SEs that are produced from the alkene group from the diallylammonium collide primarily with the Cr atoms (due to it having a larger scattering cross section than the surrounding atoms) in the resist and cause a cascade of SEs that are emitted from the Cr atoms. These electrons are produced at a reduced electron energy than that of the incident electron beam and have a greater probability of interaction with the atoms (C, H, O) that make up the pivalate molecules in the outer region of the resist. The pivalates on the outside of the molecule will be cleaved by the SEs, and this renders the resist insoluble in the developing solvent and has the effect of reducing the exposure dose while maintaining resolution.

One of the key parameters when designing a new resist is its density. Increasing the density reduces the effective mean free path of the electrons. Therefore, the electron will experience more collisions due to the reduced distance in between the atoms. This increases the probability of emitting SEs from the atoms with a high density into the immediate exposure area of the resist film. Clearly, as more SEs are generated, it means an increase in resist sensitivity, but this comes at the expense of resolution. To overcome this, the resolution can be controlled by the molecular weight of the resist molecule. The larger the molecular weight, the fewer the positions at which the electrons can have a scatter interaction with the resist. It is important to recognize that these resists do not behave like polymers such as poly meth methyl acrylate (PMMA) or ZEP520A. Our resists have a very large molecular weight (>2000 g/mol, while a PMMA monomer is 102 g/mol as the electrons do not see the entire PMMA chain) with a low density, hence the large hole in the middle. So there is more free space than resist matter for the electrons to scatter from. The addition of the dopant (mercury-based compounds) increases the density at that localized position. This means that the resist molecule is partially rendered insoluble in the developing solvent as the electrons expose this area first as less electrons are required to produce the pattern. Hence, the SEs are confined to the immediate exposure area of the pattern. Thus, producing high-resolution patterns. From an ecological point of view, incorporating mercury dichloride and mercury diiodide products to the resist chemistry sounds like something that would not be good for the environment. Using these products causes the resist insoluble in all polar solvents and is only soluble nonpolar solvents, such as tert butyl methyl ether, diethyl ether, and hexanes. This makes it easy to handle and the resist can be easily be tracked and recovered from the

Downloaded From: https://www.spiedigitallibrary.org/journals/Journal-of-Micro/Nanopatterning,-Materials,-and-Metrology on 07 Jun 2022
Terms of Use: https://www.spiedigitallibrary.org/terms-of-use

spinner for future use. Also, it should be noted that when bound to the C_7NiF_8 ring, the quantity of mercury dichloride and mercury diiodide is very low, where there is a presence of 11% and 21% of the molecule, respectively.

Preliminary EBL studies led us to study a resist using electrons and EUV as the exposure method that is based on a metal-organic compound $[NH_2(CH_2{-}CH{=}CH_2)_2][Cr_7NiF_8(O_2C^tBu)_{16}]$ **1** where seven chromium(III) centers (in green in Fig. 1) and nickel(II) (in green with a blue band in Fig. 1) form an octagon.[7] The exterior of the compound consists entirely of *tert*-butyl groups, and this gives the compound a high solubility in solvents suitable for preparing films on silicon substrates. The compound has a density ($\rho = 1.212\ \mathrm{g\,cm^{-3}}$) with a large molecular weight (2192 Da). The resist forms a closely packed film when it is spun on the silicon substrate. This is a high-resolution but low-sensitivity resist.

To improve the sensitivity, we functionalized the resist **1** with an *iso*-nicotinate ($O_2CC_5H_4N$) group that can then be bound to mercury dichloride ($HgCl_2$) to give $[NH_2(CH_2{-}CH{=}CH_2)_2][Cr_7NiF_8(O_2C^tBu)_{15}(O_2CC_5H_4N{-}HgCl_2)]$ [resist **2** in Fig. 1(b)]. The compound has a density ($\rho = 1.7\ \mathrm{g\,cm^{-3}}$) with a large molecular weight (2484 Da). We hypothesized that the mercury dichloride would increase the resist sensitivity because it would generate low-energy SEs upon absorbing the EUV radiation. These SEs will create a chain reaction of cascading electrons that will expose the resist in the immediate exposure area.

To further increase the resist sensitivity, we hypothesized that substituting the mercury dichloride in resist **2** for a mercury diiodide would give the resist a stronger atomic absorption cross-section to EUV radiation due to the presence of iodine within the molecule.[8] This was achieved by functionalizing **1** with an *iso*-nicotinate ($O_2CC_5H_4N$) group that can then be bound to mercury diiodide (HgI_2) to give $[NH_2(CH_2{-}CH{=}CH_2)_2][Cr_7NiF_8(O_2C^tBu)_{15}(O_2CC_5H_4N{-}HgI_2)]$ **3** [Fig. 1(c)]. The compound has a density ($\rho = 2.1\ \mathrm{g\,cm^{-3}}$) with a large molecular weight (2667 Da).

We used our Excalibur Monte Carlo simulator to understand the lithographic sensitivity performance of these resists materials. Figure 2 shows 3D scattering trajectory plots, first they demonstrate that all of the resists confine the primary electrons to the immediate write area which suggested that high-resolution nanostructures could be obtained for each resist. Second, they showed that the introduction of the diallylammonium and $HgCl_2$ and HgI_2 molecule to resists **2** and **3** generates more SE than resist **1** in the resist. It was calculated that resist **1** produced 11,114 SEs while resists **2** and **3** produced 24,451 and 40,010, respectively. Therefore, it is expected that the dose required to render the resist insoluble should be ~2.2 and 3.6 times lower than resist **1**. This is important, as these electrons are responsible for exposing the resist, and they subsequently increase the overall sensitivity while contributing to the proximity effect.

EBL and EUVL exposures were performed on silicon wafers of $20 \times 20\ \mathrm{mm^2}$. Each resist (15 mg) was dissolved in tert butyl methyl ether (2 g). Each solution was filtered using a 0.2-μm polytetrafluoroethylene syringe filter and was spin-coated with a spin rate of 6000 rpm for 30 s, followed by a 100°C soft bake for 2 min. The resulting thickness was measured to be 30 nm.[2]

The EBL experiments were performed using a Raith EPBG5200. The exposure clearing dose of each resist was determined using a one-dimensional matrix of single-pixel-wide lines with HP 22.5 and 15 nm HP and were 5 μm long. The current and step sizes used were 100 pA and 5 nm for the 100 keV exposures, respectively. The patterns were exposed in sets of 10 lines with one pass of the beam per line, and the line dose of each set ranged from 2000 to 30,000 $\mu\mathrm{C/cm^2}$ with incremental steps of 100 $\mu\mathrm{C/cm^2}$.

The EUVL experiments were performed using an EUV interference lithography (EUV-IL) technique at the XIL-II beamline at the Swiss Light Source of the Paul Scherer Institute.[9] The provided spatially coherent beam was tuned at an energy of 92 eV (13.5 nm wavelength) with 4% bandwidth and the measured photon flux was 34 $\mathrm{mW/cm^2}$. Each resist material was exposed through a photomask that consisted of patterns of lines and spaces with HP of 22 and 16 nm. To determine the optimum exposure dose, the dose was modified by varying the exposure time that radiation was incident on the resist. The exposure dose ranged from 100 to 2000 $\mathrm{mJ/cm^2}$. Following both lithography methods, each resist was developed in hexane for 10 s to dissolve away the unexposed resist, then blow-dried with nitrogen.

To predict the potential behavior of each resist with EUV radiation. We have used the x-ray interacts with matter CRXO database[10] to calculate the absorption coefficient of each resist.

Downloaded From: https://www.spiedigitallibrary.org/journals/Journal-of-Micro/Nanopatterning,-Materials,-and-Metrology on 07 Jun 2022
Terms of Use: https://www.spiedigitallibrary.org/terms-of-use

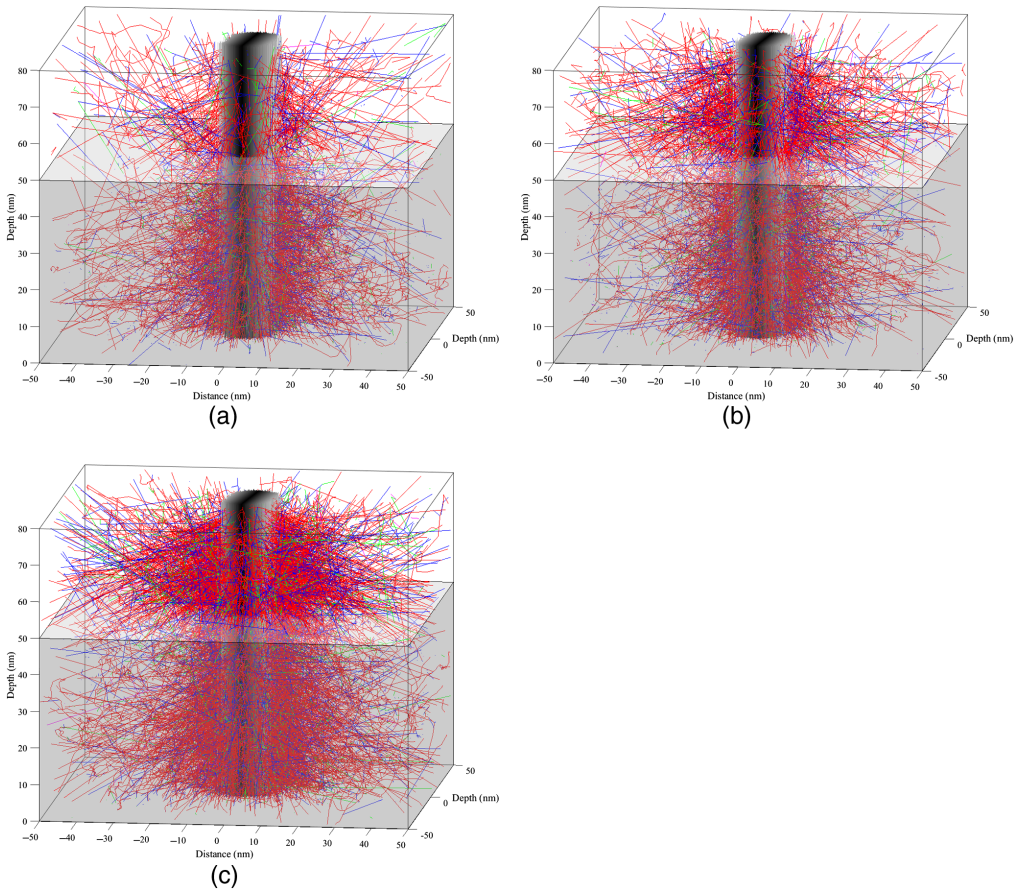

Fig. 2 Point spread function of the internal electron scattering interactions inside 30-nm films of: (a) resist **1**, (b) resist **2**, and (c) resist **3**. The acceleration voltage is 100 KeV. The black lines represent the primary electrons from the incident beam while the SEs above 500 eV are represented by the red lines. The SEs that have the associated energies below 500 eV, which were generated by first-, second-, and third-order collisions, are indicated purple, cyan, and green. The blue lines are backscattered electrons; 1 million electrons are inserted into a single spot.

It was calculated that resists **1**, **2**, and **3** had an absorption coefficient of 4.93×10^7 cm^{-1}, 6.18×10^7 cm^{-1}, and 8.03×10^7 cm^{-1}, respectively. From this, it was determined that the sensitivity of resist **3** should be at least 1.6 times more sensitive than resist **1** and resist **2** should be at least 1.25 times more sensitive to the EUV radiation than resist **1**. It should be pointed out that this only shows how much each resist absorbs the EUV radiation and does not account for the internal mechanism of producing SE's cascade which also exposes the resist. Therefore, it would be expected that the sensitivity difference between each resist should be larger.

The scanning electron microscope (SEM) images seen in Fig. 3 show 22.5 and 15 nm HP lines in all three resists, patterned using EBL. The patterns are all well-resolved and demonstrate good line uniformity.

At first glance, it appears that all of the nanopatterns in the SEM images are the same for all resist materials as expected. The difference is the exposure dose that is required to partially render each resist insoluble in the developer, which is hexane. The exposure dose that is required to expose each resist is significantly reduced when functionalizing resist **1** with HgI_2 to give **3**. It can be seen that the pattern resolution has not changed because the resist design rules (large density and large molecular weight to obtain high-resolution nanostructures) that govern the pattern were met.

It is important to understand the mechanism to how the features are resolved. To do this we must first determine how far the SEs travel with the resist. We can do this by determining how they are deposited within the resist and more importantly, what are their associated energies are

Downloaded From: https://www.spiedigitallibrary.org/journals/Journal-of-Micro/Nanopatterning,-Materials,-and-Metrology on 07 Jun 2022
Terms of Use: https://www.spiedigitallibrary.org/terms-of-use

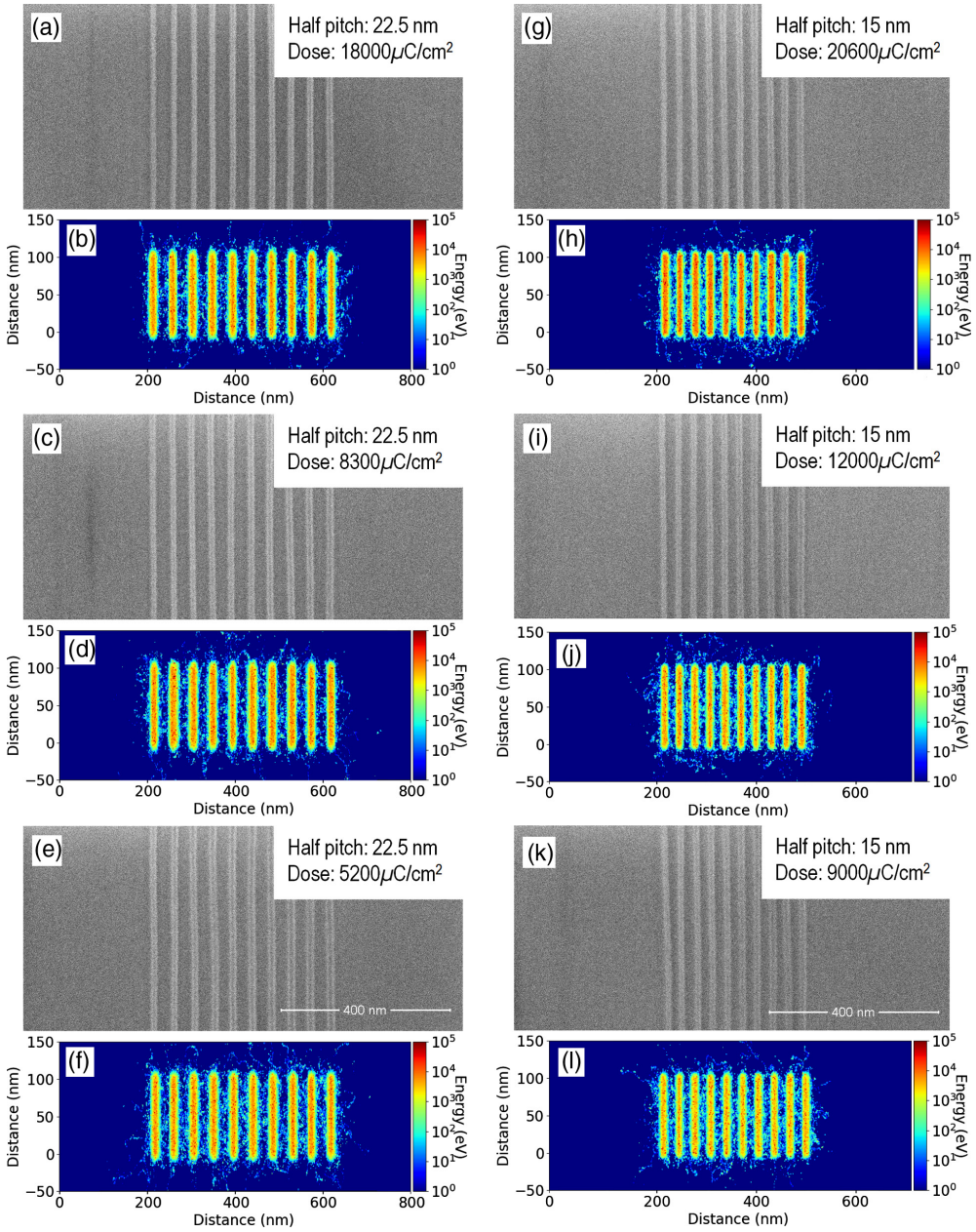

Fig. 3 (a) Scanning electron micrograph of EBL exposures with 22.5-nm HP lines fabricated in resist **1**; (b) Monte Carlo simulation of SEs energy deposited in resist **1** using 100 KeV acceleration voltage with 109,180 incident electrons per spot; (c) scanning electron micrograph of EBL exposures with 22.5-nm HP lines fabricated in resist **2**; (d) Monte Carlo simulation of SEs energy deposited in resist **2** using 100 KeV acceleration voltage with 50,547 incident electrons per spot; (e) scanning electron micrograph of EBL exposures with 22.5-nm HP lines fabricated in resist **3**; (f) Monte Carlo simulation of SEs energy deposited in resist **3** using 100 KeV acceleration voltage with 315,549 incident electrons per spot; (g) scanning electron micrograph of EBL exposures with 15 nm HP lines fabricated in resist **1**; (h) Monte Carlo simulation of SEs energy deposited in resist **1** using 100 KeV acceleration voltage with 124,950 incident electrons per spot; (i) scanning electron micrograph of EBL exposures with 15-nm HP lines fabricated in resist **2**; (j) Monte Carlo simulation of SEs energy deposited in resist **2** using 100 KeV acceleration voltage with 73,070 incident electrons per spot; (k) scanning electron micrograph of EBL exposures with 15 nm HP lines fabricated in resist **3**; (l) Monte Carlo simulation of SEs energy deposited in resist **3** using 100 KeV acceleration voltage with 54,326 incident electrons per spot.

Downloaded From: https://www.spiedigitallibrary.org/journals/Journal-of-Micro/Nanopatterning,-Materials,-and-Metrology on 07 Jun 2022
Terms of Use: https://www.spiedigitallibrary.org/terms-of-use

as they travel through the resist. From this, we can ascertain what the probability of an interaction with the resist would be. The lower their energy, the more damage in the immediate exposure area will be. To determine this, we have tracked the SEs generated while retaining their associated energy and we created energy deposition plots.

It can be seen from the simulations that patterns with features of 22.5 and 15 nm HP were be resolved. At first glance, it appears that all the simulations appear to be the same, and that is the point. The difference is the number of electrons that reflected the dose [shown in Figs. 3(a), 3(c), 3(e), 3(g), 3(i) and 3(k)] was required to fully render each resist insoluble in the developer.

The simulations show that as the width of line gets larger, the energy toward the edge of the feature reduces significantly. It is clear that the energy of the electrons in the middle of the feature starts as 100 KeV (which is the incident energy of the PE) and over a distance of 7.5 nm (for the case of 15 nm HP features, Figs. 3(h), 3(j), and 3(l)] the energy of the SEs essentially is <10 eV. The distance that the majority of SEs travel is significantly less than 10 nm. It shows that the stopping power of both $HgCl_2$ and HgI_2 dopants in resists **2** and **3** confines the SE to immediate exposure area.

The SEM images in Fig. 4 show nanopatterns obtained with EUVL with lines and spaces with 22 and 16 nm HP in all three resists. The patterns are fully resolved in all resists and demonstrate good line uniformity. Like the EBL experiments, all of the patterns appear to be the same and follow the same reduction of exposure doses that are required to render each of the resists insoluble to the hexane solvent. It was determined that the doses required to expose resists **1**, **2**, and **3** were 534, 228, and 152 mJ/cm^2, respectively, to produce a pattern with an HP of 22 nm, while to produce a pattern with an HP of 16 nm, the required doses for resists **1**, **2**, and **3** were 625, 322, and 244 mJ/cm^2, respectively.

The bridging seen in Fig. 4(d) is due to that the exposure latitude of the resist and when performing the experiment the exposure dose was on the high end of the dose scale.

Figure 5(a) shows the exposure doses required to produce the patterns shown in Figs. 3 and 4. It is evident that the presence of $HgCl_2$ in **2** and HgI_2 in **3** decreases the exposure dose, demonstrating that we have chemical control of the exposure dose. Thus, for the EBL experiment,

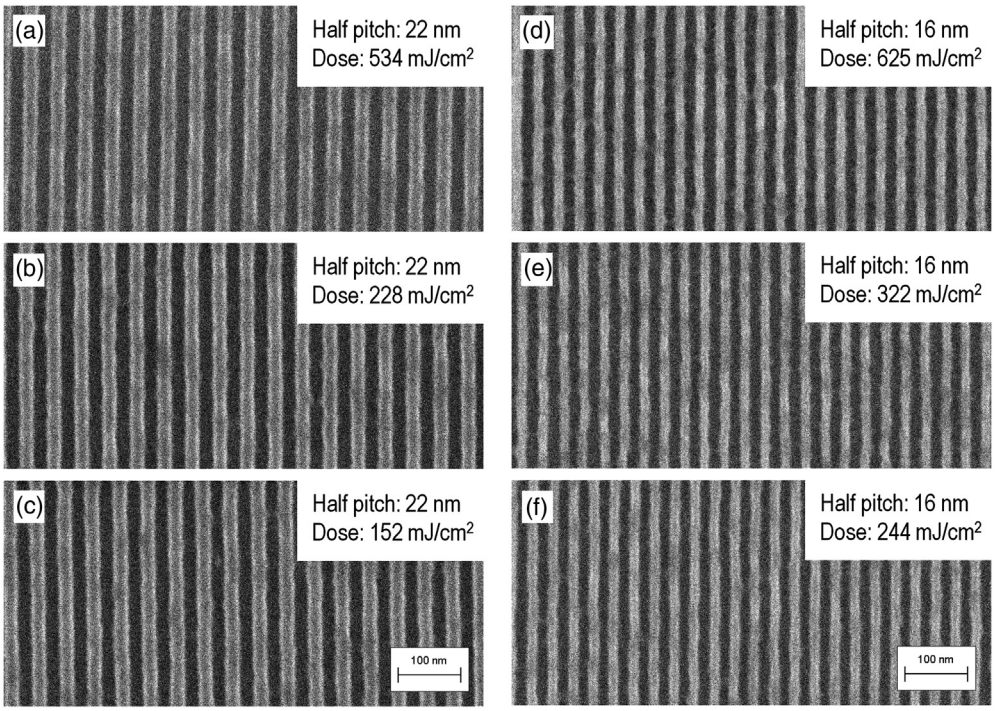

Fig. 4 (a) Scanning electron micrograph of patterns of 22 nm HP lines fabricated in resist **1**; (b) in resist **2**; and (c) in resist **3**. (d) Scanning electron micrograph of developed patterns of 16 nm HP lines fabricated in resist **1**, (e) resist **2**, and (f) resist **3**.

Downloaded From: https://www.spiedigitallibrary.org/journals/Journal-of-Micro/Nanopatterning,-Materials,-and-Metrology on 07 Jun 2022
Terms of Use: https://www.spiedigitallibrary.org/terms-of-use

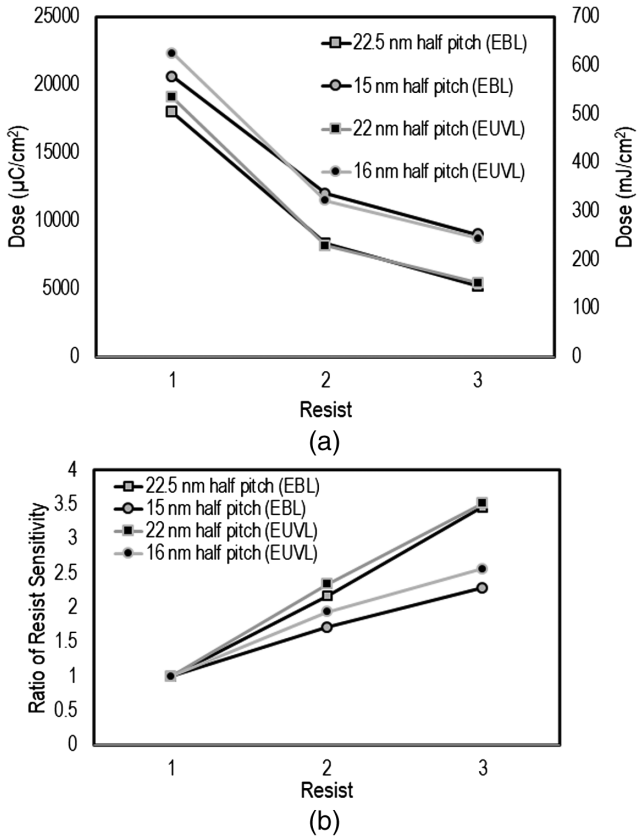

Fig. 5 (a) Dose-to-clear values for all resist materials using EUVL and EBL. (b) Relative of the sensitivity of the resists for EUVL and EBL.

it can be seen from Fig. 5(b) that the dose required for **3** decreases by a factor of 3.4 and 2.3 times when compared with **1** for the 22.5 and 15 nm HP, respectively, and this matches the Monte Carlo simulations of Fig. 2 for an HP of 22.5 nm. The Monte Carlo simulation was demonstrated using a single point, and the proximity effect was not accounted for, thus, the dose factor for the higher pitch is lower. In the EUVL experiment, the dose required for **3** is reduced by a factor of 3.5 and 2.5 times when compared with **1** for the 22 and 16 nm HP, respectively. This sensitivity increase is greater than what was predicted by the absorption coefficient calculations. This shows that the generation of SEs contributes to increasing the sensitivity.

The immediate observation is that the addition of HgI_2 in resist **3** increases the sensitivity of the resist by 2.3 or 2.5 times for EBL and EUVL at an HP of 15 and 16 nm respectively, compared with **1**. For EBL, resist **3** was determined to be 1.3 times more sensitive than resist **2** for both pitches shown. The design of the resist was based upon density and differed by a factor of 1.2. This means that the probability of the incident electrons colliding with the HgI_2 to produce SEs is higher than that of $HgCl_2$. Whereas the density difference between resist **1** and **3** is 1.7; however, the sensitivity difference between resist **1** and **3** is 3.4 and 2.3 for 45 and 30 pitches, respectively. It must be noted that the molecular weight of resist **1** is 1.2 times smaller than resist **3** and this accounts for the reduction of the sensitivity.

For EUVL, the exposing mechanism is based upon the metals, and in **3** iodine, absorbing the radiation and emitting SEs into the immediate exposure area. Resist **3** has mercury diiodide bound to the outside of the molecule and the atomic absorption cross-section associated with iodine is one of the strongest of all of the elements on the periodic table.

This gives rise to producing SEs which will collide with the Hg atom in the resist and cause a cascade of SEs that are emitted from the Hg atoms. These electrons will cleave the pivalates on the outside of the molecule which are close to the HgI_2 site. This renders the resist partially insoluble in the developing solvent and has the effect of reducing the exposure dose while maintaining resolution. Clearly, resists **1** and **2** do not have any iodine present. The mercury atomic

Downloaded From: https://www.spiedigitallibrary.org/journals/Journal-of-Micro/Nanopatterning,-Materials,-and-Metrology on 07 Jun 2022
Terms of Use: https://www.spiedigitallibrary.org/terms-of-use

absorption cross-section is 2.1 times lower than that of the iodine.[8] Therefore, it is expected that the resist sensitivity of **2** when compared with **3** should be lower by a factor of 2.

It was determined that the resist sensitivity difference between them is 1.5 and 1.3 for 22 and 16 nm HP, respectively. Resist **1** does not have any Hg or I in the resist and the Cr atomic absorption cross-section is 2.6 and 5.4 times lower than the atomic absorption cross-section of mercury and iodine atoms, respectively.[8] It was determined that the resist sensitivity is lower by a factor of 3.5 and 2.5 with respect to 22 and 16 nm HP. The discrepancy may be based on the feature size of the pattern because the probability of the landing of an EUV photon in the exposure area is lower with increasing resolution; and therefore, it will need more photons to interact with the resist molecule. Also, other atoms of the resist molecule may dominate and absorb the photons, which lowers the effect of the iodine. It is clear that the sensitivity discrepancies observed warrant further investigation.

From the results shown here, it is clear that the exposure sensitivity does not seem to be dependent upon the exposing medium used as the difference in sensitivity demonstrated with resist **3** when compared with resist **1** is the same for EBL and EUVL.

2 Conclusions

Three metal-organic negative tone resists have been investigated by EBL and EUVL. We have demonstrated that the exposure sensitivity of the materials can be increased by 2.3 and 2.5 times for the EBL and EUVL studies by chemical design, i.e., by introducing components such as mercury diiodide in **3** while maintaining a high resolution of 15 and 16 nm HP, respectively. The good correlation between EBL and EUVL is perhaps surprising, given that the energy of the incident electrons and photons is different. For EUVL the radiation has energy of 92 eV and with EBL we are exposing at 100 keV. The reason for the correlation is that in each case the energy is sufficient to excite SEs from the resist material; EBL is in fact more energetic than it needs be to excite SEs from any element. For EUV, the controlling factor is the EUV cross-section of the elements present but there is still enough energy to excite SEs (the energy of these electrons is 20 eV and below), which control the exposure sensitivity. This contrast with longer wavelength photolithography where the exciting radiation is breaking covalent bonds through excitations.

Acknowledgments

We acknowledge the EPSRC (UK) for funding (Grant No. EP/R023158/1) and Innovate UK for funding (project 72472). The University of Manchester also supported this work. The authors gratefully acknowledge the critical support and infrastructure provided for this work by the Kavli Nanoscience Institute at Caltech. REPW thanks the European Research Council for an Advanced Grant (ERC-2017-ADG-786734) and the EPSRC (UK) for an Established Career Fellowship (EP/R011079/1). This project has received funding from the EU-H2020 research and innovation program under Grant Agreement No. 654360 having benefitted from the access provided by PSI in Villigen within the framework of the Nanoscience Foundries and Fine Analysis Europe Transnational Access Activity. The manuscript was written through the contributions of all authors. All authors have given approval to the final version of the manuscript. These authors contributed equally; Scott M. Lewis designed the research and wrote the manuscript, Hayden R. Alty designed and programmed the Excalibur Monte Carlo Simulator software, Michaela Vockenhuber ran the XIL beamline at the PSI and performed the EUV exposures on the photoresists, Dimitrios Kazazis performed the EUV exposures and acquired the SEM images of the photoresist. Paul. L. Winpenny designed and programmed the pattern analysis software, Guy A. Derose provided the EPBG5200 EBL tool and fabricated the patterns, Axel Scherer provided the EPBG5200 EBL tool and lab facilities necessary to verify the results, Yasin Ekinci provided the XIL beam EUV exposure tool and lab facilities necessary to verify the results. Grigore A. Timco and Richard Grindell made the compounds studied. Richard E. P. Winpenny provided the chemistry facilities and lab infrastructure. EPSRC (UK) Grant EP/R023158/1; Innovate UK project 72472; European Research Council ERC-2017-ADG-786734; EPSRC (UK) EP/R011079/1.

Downloaded From: https://www.spiedigitallibrary.org/journals/Journal-of-Micro/Nanopatterning,-Materials,-and-Metrology on 07 Jun 2022
Terms of Use: https://www.spiedigitallibrary.org/terms-of-use

References

1. More Moore, "IEEE international roadmap for devices and systems," 2018, www.irds.ieee.org (accessed 03/02/2020).
2. S. Lewis et al., "Design and implementation of the next generation electron beam resists for the production of EUVL photomasks," *Proc. SPIE* **10810**, 108100N (2018).
3. S. M. Lewis et al., "Plasma-etched pattern transfer of sub-10 nm structures using a metal-organic resist and helium ion beam lithography," *Nano Lett.* **19**, 6043−6048 (2019).
4. S. M. Lewis and G. A. DeRose, *Frontiers of Nanoscience, Materials and Processes for Next Generation Lithography: SML Electron Beam Resist: Ultra-High Aspect Ratio Nanolithography*, Vol. 11, pp. 421–446, Elsevier (2016).
5. S. M. Lewis et al., "Use of supramolecular assemblies as lithographic resists," *Angew. Chem.* **129**(24), 6853–6856 (2017).
6. B. Wu and A. R. Neureuther, "Energy deposition and transfer in electron-beam lithography," *J. Vac. Sci. Technol. B: Microelectron. Nanometer Struct. Process. Meas. Phenom.* **19**, 2508 (2001).
7. G. F. S. Whitehead et al., "A ring of rings and other multicompoment assemblies of cages," *Angew. Chem. Int. Ed.* **52**, 9932–9935 (2013).
8. R. Fallica et al., "Absorption coefficient of metal containing photoresists in the extreme ultraviolet," *J. Micro/Nanolithogr. MEMS MOEMS* **17**(2), 023505 (2018).
9. C. Popescu et al., "Sensitivity enhancement of the high resolution xMT multi-trigger resist for EUV lithography," *Proc. SPIE* **10143**, 101430V (2017).
10. B. L. Henke, E. M. Gullikson, and J. C. Davis, "X-ray interactions: photoabsorption, scattering, transmission, and reflection at E = 50–30000 eV, Z = 1–92," *At. Data Nucl. Data Tables* **54**(2), 181–342 (1993).

Scott M. Lewis is a research fellow at the University of Manchester. He received his BEng, MSc degrees, and a PhD in electronic engineering from Cardiff University in 2002, 2004, and 2009, respectively. His research focuses on developing new Monte Carlo models to design new resist materials and in nanofabrication by photo and e-beam lithography. He holds the prestigious position of visiting associate researcher at the California Institute of Technology.

Biographies of the other authors are not available.

Downloaded From: https://www.spiedigitallibrary.org/journals/Journal-of-Micro/Nanopatterning,-Materials,-and-Metrology on 07 Jun 2022
Terms of Use: https://www.spiedigitallibrary.org/terms-of-use